

Article

Green Synthesis of Copper Oxide Nanoparticles Using Protein Fractions from an Aqueous Extract of Brown Algae *Macrocystis pyrifera*

Karla Araya-Castro ^{1,2} , Tzu-Chiao Chao ³, Benjamín Durán-Vinet ² , Carla Cisternas ¹, Gustavo Ciudad ⁴ and Olga Rubilar ^{4,*}

¹ Doctoral Program in Science of Natural Resources, Universidad de La Frontera, Temuco 54-D, Chile; karla.araya@ufrontera.cl (K.A.-C.); carla.cisternas@ufrontera.cl (C.C.)

² Scientific and Technological Bioresource Nucleus, Universidad de La Frontera, Temuco 54-D, Chile; b.duran01@ufromail.cl

³ Institute of Environmental Change & Society, Department of Biology, University of Regina, Regina, SK S4S, Canada; tzu-chiao.chao@uregina.ca

⁴ Chemical Engineering Department, Universidad de La Frontera, Temuco 54-D, Chile; gustavo.ciudad@ufrontera.cl

* Correspondence: olga.rubilar@ufrontera.cl

Abstract: Amongst different living organisms studied as potential candidates for the green synthesis of copper nanoparticles, algal biomass is presented as a novel and easy-to-handle method. However, the role of specific biomolecules and their contribution as reductant and capping agents has not yet been described. This contribution reports a green synthesis method to obtain copper oxide nanoparticles (CuO-NPs) using separated protein fractions from an aqueous extract of brown algae *Macrocystis pyrifera* through size exclusion chromatography (HPLC-SEC). Proteins were detected by a UV/VIS diode array, time-based fraction collection was carried out, and each collected fraction was used to evaluate the synthesis of CuO-NPs. The characterization of CuO-NPs was evaluated by Dynamic Light Scattering (DLS), Z-potential, Fourier Transform Infrared (FTIR), Transmission Electron Microscope (TEM) equipped with Energy Dispersive X-ray Spectroscopy (EDS) detector. Low Molecular Weight (LMW) and High Molecular Weight (HMW) protein fractions were able to synthesize spherical CuO-NPs. TEM images showed that the metallic core present in the observed samples ranged from 2 to 50 nm in diameter, with spherical nanostructures present in all containing protein samples. FTIR measurements showed functional groups from proteins having a pivotal role in the reduction and stabilization of the nanoparticles. The highly negative zeta potential average values from obtained nanoparticles suggest high stability, expanding the range of possible applications. This facile and novel protein-assisted method for the green synthesis of CuO-NPs may also provide a suitable tool to synthesize other nanoparticles that have different application areas.

Keywords: green synthesis; brown seaweed; proteins; size exclusion chromatography; copper oxide nanoparticles



Citation: Araya-Castro, K.; Chao, T.-C.; Durán-Vinet, B.; Cisternas, C.; Ciudad, G.; Rubilar, O. Green Synthesis of Copper Oxide Nanoparticles Using Protein Fractions from an Aqueous Extract of Brown Algae *Macrocystis pyrifera*. *Processes* **2021**, *9*, 78. <https://doi.org/10.3390/pr9010078>

Received: 11 December 2020

Accepted: 28 December 2020

Published: 31 December 2020

Publisher's Note: MDPI stays neutral with regard to jurisdictional claims in published maps and institutional affiliations.



Copyright: © 2020 by the authors. Licensee MDPI, Basel, Switzerland. This article is an open access article distributed under the terms and conditions of the Creative Commons Attribution (CC BY) license (<https://creativecommons.org/licenses/by/4.0/>).

1. Introduction

The eco-friendly synthesis of nanoparticles (NPs) is a challenging field in nanobiotechnology and is presented as a promising alternative to chemical pathways since it avoids the production of secondary contaminants that are affecting the environment [1,2]. The green synthesis of NPs uses reductant agents from bacteria, yeast, plants, algae, fungi or plants, which contain secondary metabolites, such as sugars, alginates, proteins, some amino acids, and other molecules used to reduce metals in order to generate reduced ions that lead the nucleation process [3]. As a second step, the capping process may also be performed by biological agents, such as proteins, instead of chemicals, such as polyvinylpyrrolidone (PVP), to stabilize the nucleation process and obtain long-term stable NPs [4,5].

Those environment-friendly and cost-effective methods produce NPs of different compositions, sizes, morphologies, and dispersion, which may affect their final property and application [6–8]. The interest in copper-based NPs is given to their optical, conducting, magnetic, catalytic, thermal, and antibiotic activity, owing to the enhanced physico-chemical properties due to their small surface to volume ratio when compared to its bulk material [9,10]. The use of raw aqueous algal extracts has been explored by a few authors as reductant and capping sources for the green synthesis of Cu-NPs [11–15]. In this context, copper oxide nanoparticles (CuO-NPs) have been successfully synthesized using a boiled aqueous extract from the brown algae *Bifurcaria bifurcata* and *Cystoseira trinodis* within a size range from 5 to 45 nm and 6 to 7.8 nm, respectively [11,14]. In addition, an aqueous extract from brown seaweed (*Sargassum polycystum*) was used by Ramaswamy et al. [13] to produce CuO-NPs. In a similar way, an autoclaved aqueous extract from the green microalgae *Botryococcus braunii* produced CuO-NPs in a size range between 10 and 70 nm [12]. Alternatively, Bhattacharya et al. [15] performed a slightly different method by heating at 50 °C instead of boiling the extract in order to get an aqueous extract from the microalgae *Anabaena cylindrica*, and CuO-NPs with a particle size of 3.6 nm were obtained. It is important to note that a detailed characterization of the components of algae responsible for the reduction and stabilization process using copper as promotor is yet to be discovered. Therefore, it is relevant to lead studies towards using specific biomolecules in the green synthesis on CuO-NPs in order to expand their use for biological applications. This also may provide a better understanding to portrait its impact on the main characteristics of the CuO-NPs.

Here, we report a rapid and green synthesis method to obtain CuO-NPs using HPLC-size exclusion chromatography (SEC) separated protein fractions from an aqueous extract of the brown algae *Macrocystis pyrifera* as a reductant and capping agent. Our study suggests that using water-soluble proteins from *M. pyrifera* represents a consistent, straightforward green method to synthesize homogenous nanoscale size CuO-NPs that exhibits high-stability.

2. Materials and Methods

Brown Marine *Macrocystis pyrifera* algae were obtained from Universidad de Los Lagos; samples were collected in Quenac, Chiloé Island, (Chile). In order to remove epiphytes and sand particles, biomass was washed three times with tap water, then twice with distilled water, and followed by twice-double deionized water. Subsequently, algal biomass was dried in an oven at 50 °C overnight. The dried biomass was powdered in a blender and stored in darkness. A 100 mM CuSO₄ (Loba Chemie, Mumbai, India) was prepared using double distilled water and kept at 4 °C in the dark for further experiments.

2.1. Preparation of *Macrocystis pyrifera* Biomass-Free Non-Boiled (BFNB) Extract and Protein Precipitation from the Algal Aqueous Extract

Dried algal powder (4 g) was dispersed in a 250 Erlenmeyer flask with 100 mL double distilled water, sonicated for 15 min (VCX 130, SONICS) at 60% amplitude to facilitate cell lysis [16], and incubated in an orbital shaker (200 rpm) for 24 h at 50 °C. Once cooled, the supernatant was separated from the biomass by centrifugation at 4000 rpm for 20 min, and two volumes of cold acetone (Merck, Darmstadt, Germany); were added to the previously obtained aqueous extract in a 50 mL centrifuge tube. The mix was vortexed thoroughly and incubated overnight at −20 °C. Samples were centrifuged at 4 °C for 20 min at 14,000 g, the supernatant was removed from the pellet, and 1 mL of 50 mM ammonium bicarbonate buffer (Merck, Darmstadt, Germany); was added to re-solubilize the pellet. These steps were repeated twice to ensure the removal of all undesired components from the sample. Sodium dodecyl sulfate (SDS) (Merck, Darmstadt, Germany); at a final concentration of 1% was added to dissolve remaining proteins prior to HPLC procedures.

2.2. Protein Separation by Size-Exclusion Chromatography and Quantification by BCA Assay

The samples obtained in the previous activity were analyzed by size exclusion chromatography (SEC) using a Bio SEC-5 Column (Agilent Technologies, Santa Clara, CA, USA) on an HPLC (1200 Infinity series, Agilent Technologies, Santa Clara, CA, USA) connected to a fraction collector. Proteins were detected by a UV/VIS diode array detector (DAD, detection at 280 nm wavelength) (Agilent Technologies, Santa Clara, CA, USA). Running conditions were: oven temperature 25 °C, flow rate 0.5 mL/min, run time 30 min, and 50 mM ammonium bicarbonate as the mobile phase, pH 10. Time-based fraction collection was carried out every 1 min; samples were concentrated using a vacuum centrifuge and stored at −20 °C. Bovine Serum Albumin (BSA) was used as a reference. Afterward, protein fractions were quantified using a bicinchoninic acid (BCA) protein assay kit (Thermo Scientific Pierce, Rockford, IL, USA) using BSA as a calibrant.

2.3. Biogenic Synthesis and Physico-Chemical Characterization of Copper Oxide Nanoparticles Mediated by *M. pyrifera* Proteins

Samples from the protein fraction collection were used for copper nanoparticle synthesis. Those fractions without protein content were maintained as control to measure SDS impact on CuONPs formation. Subsequently, each fraction containing proteins were mixed with copper sulfate to get a final concentration of 2 mM. Samples were incubated at 45 °C on a rotary shaker for 48 h.

The samples obtained were further characterized by measuring the hydrodynamic diameter, zeta potential, and polydispersity index (PDI) values at 25 °C using the Zetasizer Nano ZS90 System (Malvern Instruments, Malvern, UK) through Dynamic Light Scattering (DLS). To avoid aggregation, samples were sonicated for 5 s Prior to the DLS measurement, the aqueous suspensions of nanoparticles were passed through a cellulose acetate syringe driven filter unit (0.22 µm pore size). For each experiment, a glass cuvette was used containing a 500 µL sonicated sample and 1 mL double distilled water. Fourier transform infrared (FTIR) spectral analysis was used to identify the functional groups present on the surface of the copper oxide nanoparticles. The transmission spectrum was recorded using a CARY 630 FTIR (Agilent Technologies) in the frequency range of 500–4000 cm^{−1}. Lastly, transmission electron microscopy (TEM) images were obtained using a Tecnai F20 FEG-S/TEM operated (FEI, Hillsboro, OR, USA) at 200 kV accelerating voltage, equipped with an Energy Dispersive X-ray Spectroscopy (EDS) detector (FEI, Hillsboro, Oregon, US). Samples were prepared by placing a drop of sample on a 300 mesh gold grid covered by carbon formvar; excess of solution was removed by blotting with filter paper and subsequently dried in air at room temperature before imaging.

3. Results and Discussion

In this study, we first tested the ability of different size-separated protein fractions from an aqueous extract of the brown algae *M. pyrifera* for the green synthesis of CuO-NPs. We used SEC in order to obtain 11 sample fractions (see Supplementary Materials Figure S1) and measured protein content in each fraction with a BCA assay. As can be seen in Table 1, fractions 3–9 contained measurable amounts of protein ranging from 0.72 µg (fraction 9) to 13.92 µg (fraction 7). We also collected low molecular weight (LMW) fractions (10 and 11) as well as high molecular weight (HMW) fractions (1 and 2), which did not contain protein.

We tested each fraction for their ability to create NPs by each sample with 2 mM copper sulfate. The first color change indicative of copper reduction was observed at 24 h, with a slight color change from light blue to light green when pellets were observed after a spin; this phenomenon was not observed in control fractions (1–2 and 10–11). The same color change phenomenon has been observed and reported by other authors when *Pterospermum acerifolium* and *Ixora coccinea* leaf extracts were used for the synthesis of CuO-NPs [17,18]. Nevertheless, both mentioned studies were focused on the use of raw leaf extract as a reductant agent, and the role of specific biomolecules was not explored. Figure 1 shows representative TEM images of the products of the CuSO₄ reduction by different protein

fractions (3, 4, 5, 6, 7, 8, and 9) from the *M. pyrifera* aqueous extract. TEM images showed that the metallic core was between 2 and 50 nm, with spherical nanostructures present in all fractions containing proteins, while in non-protein fractions, CuO-NPs were not observed. In fraction 5 (Figure 1c), the perimeter of CuO-NPs was evidently surrounded by a layer of non-metallic material with a width of ~5 nm, suggesting that proteins are also acting as capping and stabilizing agent. EDS analysis of nanoparticles (Figure 1h) indicated the copper (Cu) composition and a strong carbon (C) signal from proteins in the synthesized nanoparticles. The gold (Au) signal is explained by the grid where the sample was deposited. Furthermore, FTIR spectral analysis provided evidence of functional groups present in CuO-NPs and is shown in Figure 2. Bands at 1638 cm^{-1} and 1540 cm^{-1} are mainly associated to C-O stretching peptide bond from amide I and N-H bending and C-N stretching vibration from amide II, respectively [19]. The peak at 3440 cm^{-1} is due to N-H and O-H stretching vibrations. Moreover, a strong signal is shown at 575 and 620 cm^{-1} , which belongs to the bending mode of the CuO bond [20].

Table 1. Protein quantification using the bicinchoninic acid (BCA) assay method, after recovery of 11 fractions obtained from the elution profile.

Fraction	Absorbance	Captured Mass ($\mu\text{g}/500\text{ uL}$)
1	0.014	0
2	0.019	0
3	0.083	6.86
4	0.059	4.24
5	0.073	5.78
6	0.096	8.31
7	0.147	13.92
8	0.086	7.22
9	0.027	0.72
10	0.015	0
11	0.014	0

It is important to note that proteins with LMW and HMW were both able to synthesize spherical CuO-NPs. Similarly, even in fractions with a low protein content as fraction 9 with $0.72\text{ }\mu\text{g}$ of proteins, spherical CuO-NPs of 2 nm diameter were found (Figure 1g). Synthesized CuO-NPs from protein fractions 4 and 6 were very similar, with sizes ranging from 2 to 10 nm, showing well-dispersed nanoparticles along the field of view (Figure 1b,d). In all protein fractions observed, the synthesized nanoparticles were homogeneous in size, and agglomeration was not observed, although, in solution, there might be more aggregation, which may interfere with DLS measurement and raise the average size.

Protein stability capacity was supported by the DLS analysis results of CuO-NPs (Figure 3), where the Zeta Potential value obtained from samples 3 to 9 were highly negative, demonstrating a high charge repulsion between nanoparticles capping agents. Samples 1, 2, 10, and 11 without protein content were used as control, which shown no measurable NPs in solution, independently of 1% SDS and copper sulfate addition. An interesting correlation was found with HMW proteins since they resulted in lower zeta potential values (fraction 3, -62.1 mV , Table S1) and relatively low PDI, suggesting that larger proteins in higher concentrations may benefit the capping process while LMW proteins are more unstable (Fraction 9, -26.1 mV , Table S1). Zeta potential values higher than $+30\text{ mV}$ or lower than -30 mV exhibit high stability [21], indicating that most protein fractions can be used to create stable dispersions. Therefore, it can be proposed that proteins are acting as reductant and capping agent, conferring stability to CuO-NPs due to a protein-layered shell. Stability is a crucial aspect of nanoparticle synthesis since the lack of sufficient stability of many nanoparticle preparations has, to some extent, hindered the development of real-world applications of nanomaterials [22].

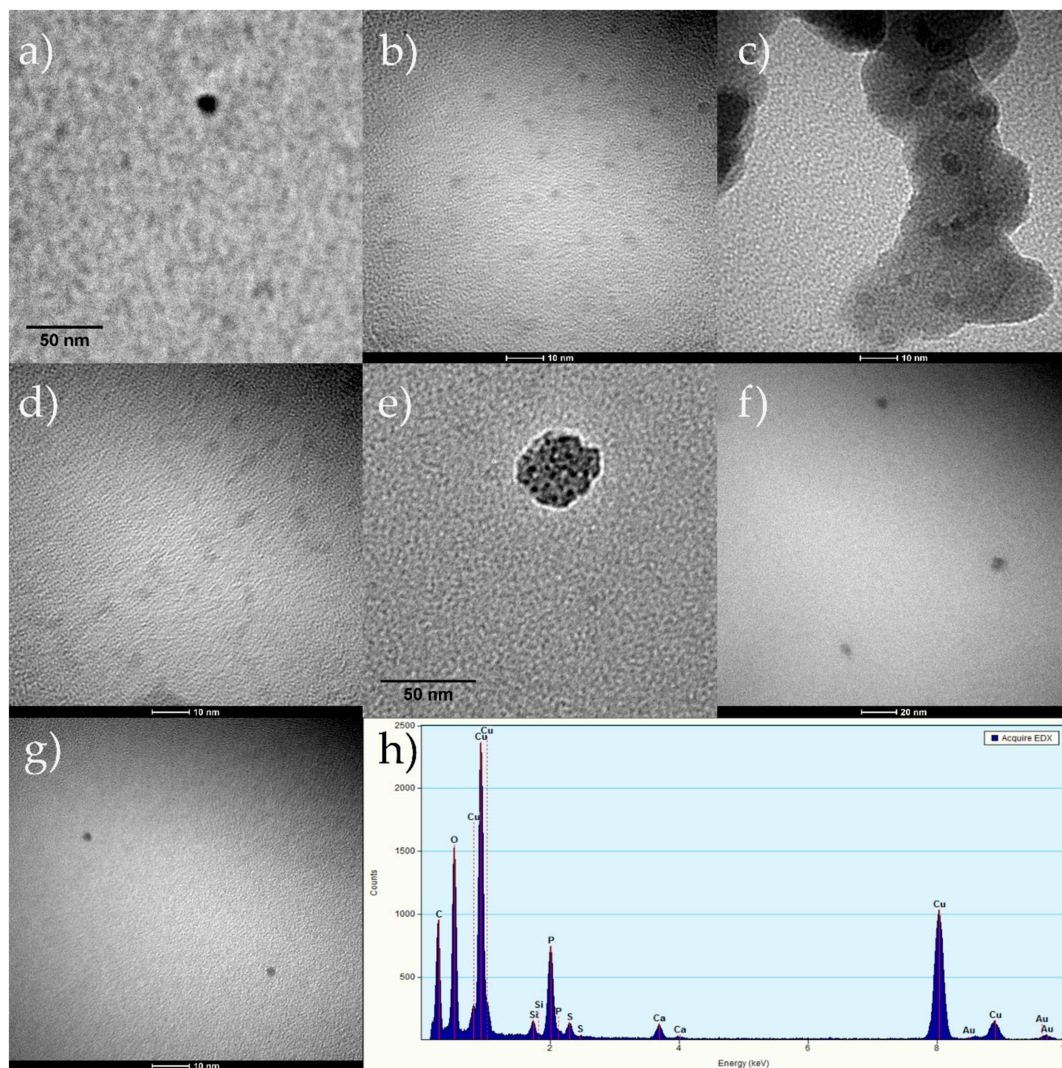


Figure 1. Transmission electron microscopy (TEM) images of the products of the CuSO_4 reduction by different protein fractions from the algal extract: (a) fraction 3; (b) fraction 4; (c) fraction 5; (d) fraction 6; (e) fraction 7; (f) fraction 8; (g) fraction 9; (h) energy dispersive spectroscopy (EDS) analysis spectrum of CuO-NPs.

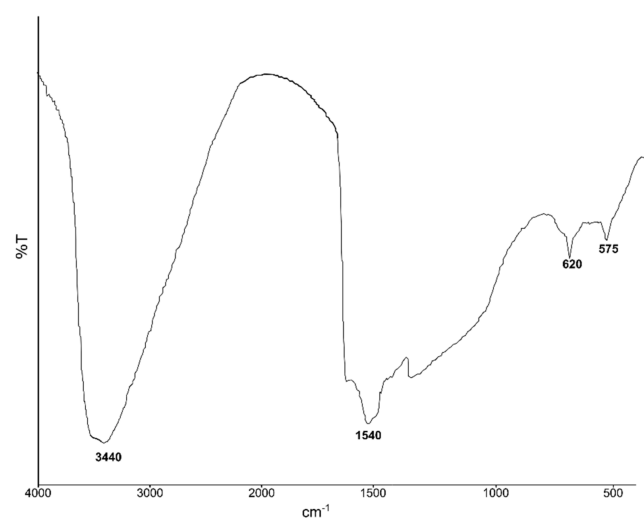


Figure 2. Fourier Transform Infrared (FTIR) spectra of CuO-NPs.

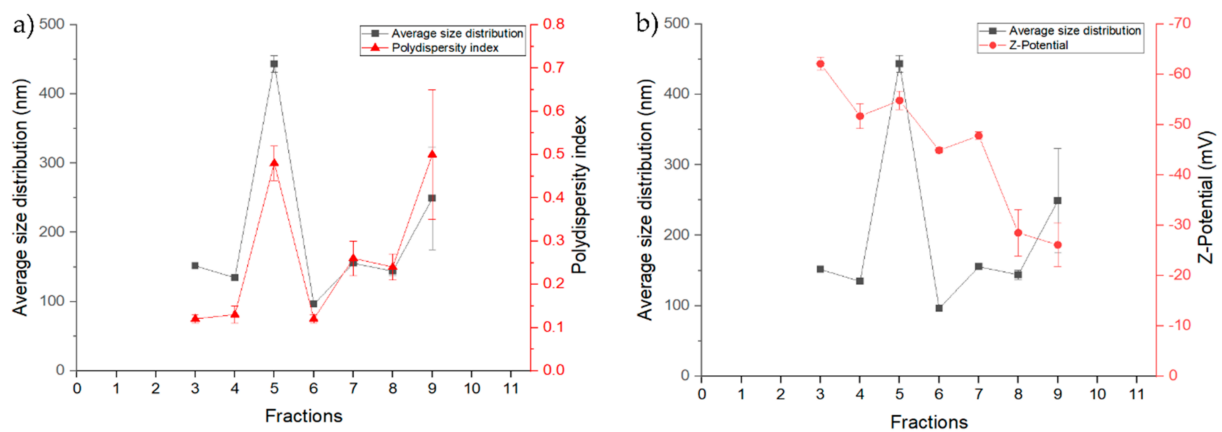


Figure 3. Characterization of CuO-NPs average size distribution, zeta potential, and polydispersity index (PDI) by Dynamic Light Scattering (DLS): (a) Average size distribution and Polydispersity index; (b) Average size distribution and Z-potential.

Results from average size distribution demonstrated nanoscale products in fractions 3, 4, 6, 7, and 8, all of them presented a PDI value below 0.3, which suggests that CuO-NPs are also highly monodispersed. Samples from fractions 5 and 9 were out of desirable size, and both PDI values are an indicative of highly polydisperse size distribution. The size difference between TEM and DLS analyses may be due to the different principles involved in these two techniques. The DLS measurement involves the hydrodynamic state of nanoparticles, whereas it is a dry state in TEM measurement [23,24].

In terms of its biochemical composition, *M. pyrifer* biomass contain 75% carbohydrates, 13% proteins, 11% ash, and 0.7% lipids [25]. Ortiz J. and collaborators [26] explored the composition of 17 amino acids in *M. pyrifer*, showing an important contribution of water-soluble amino acids, such as glutamic acid, aspartic acid, arginine, and cysteine. It has been described that biomolecules with carboxyl, hydroxyl, and amine functional groups have the potential for metal-ion reduction and for capping in the green synthesis of nanoparticles, in replacement of chemical or physical methods [27–32]. Thus, it can be explained that, even with a low protein content per fraction, glutamic, and aspartic acid represented by a various structural percentages are amino acids with significant reductant capacity at the nanoscale. Furthermore, there is strong evidence that glutamic acid and aspartic acid are capable of reducing metals for nanoparticles synthesis [33,34], while arginine has been reported as an effective capping agent of nanoparticles [35]. Moreover, all proteins that contain amino and carboxyl groups have a reported interaction with Cu^{+2} , which prevents the formed CuO-NPs from aggregating [36]. In this sense, it is relevant to note that the S signal observed in Figure 1H could indicate the presence of cysteine as a hydrophilic sulfur-containing amino acid that may lead the mechanism of reduction and stabilization for the consequent synthesis of CuO-NPs. Hence, it is suggested that these amino acids are playing a pivotal role in the generation of Cu reduced cations, along with a stabilization capacity given by the physicochemical interaction between the same proteins and the nano quant cations of reduced forms of Cu.

Moreover, a previous study identified five groups of substances present in extracellular products of different *Chlorococcum* species: (i) steam-volatile acids; (ii) yellow water-soluble phenolic compounds; (iii) lipophilic substances; (iv) proteins; and (v) polysaccharides [37]. In this aspect, FT-IR analysis of *C. humicola* silver nanoparticles revealed that protein molecules were mainly responsible for the production of biogenic silver nanoparticles, and the presence and binding of proteins with the nanoparticles could possibly lead to their stabilization. The findings of this research can be closely linked to Mohseniazar et al. [38], who demonstrated that *Nannochloropsis gaditana* and *Chlorella vulgaris* have the potential to biosynthesize silver nanoparticles in a culture medium containing silver nitrate in solution. A better characterization was done by another study whose aim was to explore the active species in the algal extract from *Chlorella vulgaris* that was responsible for the

reduction of Ag ions and the resulting growth of Ag(0) into Ag nanoplates [30]. Besides, chemical modifications of the algal proteins were carried out to identify the amino acid residues in the proteins with Ag ion reduction capability and shape direction functionality. From this analysis, the authors concluded that, in accordance with other references [39–41], algal proteins were the active biomolecules in the algal extract responsible for Ag nanoplates formation, being primarily accountable for the reduction of Ag(I) and the formation of Ag nanoplates. In addition, they discovered that Tyr residues in the proteins were responsible for Ag ion reduction, and the carboxyl groups in Asp and/or Glu residues were driving the anisotropic growth of Ag nanocrystals into nanoplates.

Studies with *Fusarium oxysporum* showed the presence of two extracellular proteins having a molecular weight of 24 and 28 kDa, which were being responsible for the synthesis of zirconia nanoparticles [41]. In conjunction with this research focus, Xie et al. [16] explored a simple and controlled biological synthesis of large quantities of gold nanoplates through room temperature reduction of gold ions for 48 h in an aqueous algal extract. Lastly, it must be mentioned that there are agents, such as FADH₂/NADH cofactors that may co-elute with the proteins, which have reported contribution as reducing agents of proteins during in vivo NPs [42], and they may be present in the fractions. However, these cofactors are unstable above pH 7. Thus, their concentration might not be significantly representative; instead, proteins are more probably leading the reducing power within samples.

The importance of this study was the identification, as far as possible, of the biomolecules involved in the nucleation and growth of gold clusters into specific shapes and sizes. For this purpose, proteins were eluted and isolated according to their molecular weight, and distinctive triangular and hexagonal gold nanoparticles obtained using a protein with approximately 28 kDa weight were purified by reversed-phase HPLC and then collected. Accordingly, results presented in this report, using protein fractions extracted from *M. pyrifera*, evidenced that both HMW and LMW proteins are capable of synthesizing CuO-NPs. However, due to differences between the fractions, there is still room for further optimization of CuO-NPs green synthesis.

4. Conclusions

This present work demonstrated a successful and straightforward strategy based on a biomolecule-assisted technique for the green synthesis of copper ion bioreduction into copper nanoparticles, using proteins precipitated from an aqueous extract of *M. pyrifera* macroalgae as both reductant and capping agent. HMW and LMW fractions were effectively used as reductant and stabilizing agent for CuO-NPs synthesis and shown some correlation between hydrodynamic size and protein size.

Reductant capacity was present in fractions with high and low protein content, indistinctively. The highly negative zeta potential average values of the obtained copper nanoparticles suggest high stability, which also showed a protein size correlation. Thus, it is fundamental to lead more research to completely elucidate biomolecules role and their impact on the green synthesis of CuO-NPs. Hence, these preliminary results on the characterization of CuO-NPs mediated by protein fractions may indeed expand the range of possible applications. This eco-friendly method should also be extendable to the preparation of different metal or biocompatible metal nanomaterials.

Supplementary Materials: The following are available online at <https://www.mdpi.com/2227-9717/9/1/78/s1>.

Author Contributions: Conceptualization, K.A.-C., G.C., and O.R.; methodology, T.-C.C. and K.A.-C.; formal analysis, T.-C.C., K.A.-C., and B.D.-V.; investigation, K.A.-C. and B.D.-V.; writing—original draft preparation, K.A.-C.; writing—review and editing, T.-C.C., C.C., and B.D.-V.; visualization, G.C.; supervision, T.-C.C., G.C., and O.R.; funding acquisition, K.A.-C., G.C., and O.R. All authors have read and agreed to the published version of the manuscript.

Funding: This research was funded by ANID Scholarship 21141234, FONDECYT project 1191239, FONDECYT project 1191089, and ANID/FONDAP/15130015.

Institutional Review Board Statement: Not applicable.

Informed Consent Statement: Not applicable.

Data Availability Statement: All data is contained within the article.

Conflicts of Interest: The authors declare no conflict of interest. The funders had no role in the design of the study; in the collection, analyses, or interpretation of data; in the writing of the manuscript; or in the decision to publish the results.

References

1. Ibraheem, I.B.M.; Abd Elaziz, B.E.E.; Saad, W.F.; Fathy, W.A. Green biosynthesis of silver nanoparticles using marine red algae *acanthophora specifera* and its antibacterial activity. *J. Nanomed. Nanotechnol.* **2016**, *7*, 7–10.
2. Makarov, V.V.; Love, A.J.; Sinitsyna, O.V.; Makarova, S.S.; Yaminsky, I.V.; Taliansky, M.E.; Kalinina, N.O. “Green” nanotechnologies: Synthesis of metal nanoparticles using plants. *Acta Naturae* **2006**, *6*, 40–61. [[CrossRef](#)]
3. Salem, S.S.; Fouda, A. Green Synthesis of metallic nanoparticles and their prospective biotechnological applications: An overview. *Biol. Trace Elem. Res.* **2020**, *199*, 344–370. [[CrossRef](#)] [[PubMed](#)]
4. Kamran, U.; Bhatti, H.N.; Iqbal, M.; Nazir, A. Green synthesis of metal nanoparticles and their applications in different fields: A review. *Z. Phys. Chem.* **2019**, *233*, 1325–1349. [[CrossRef](#)]
5. Gour, A.; Jain, N.K. Advances in green synthesis of nanoparticles. *Artif. Cells Nanomed. Biotechnol.* **2019**, *47*, 844–851. [[CrossRef](#)]
6. Albanese, A.; Tang, P.S.; Chan, W.C.W. The effect of nanoparticle size, shape, and surface chemistry on biological systems. *Annu. Rev. Biomed. Eng.* **2012**, *14*, 1–16. [[CrossRef](#)]
7. Shen, Z.; Ye, H.; Yi, X.; Li, Y. Membrane wrapping efficiency of elastic nanoparticles during endocytosis: Size and shape Matter. *ACS Nano* **2019**, *13*, 215–228. [[CrossRef](#)]
8. Banerjee, A.; Qi, J.; Gogoi, R.; Wong, J.; Mitragotri, S. Role of nanoparticle size, shape and surface chemistry in oral drug delivery. *J. Control. Release* **2016**, *238*, 176–185. [[CrossRef](#)] [[PubMed](#)]
9. Huang, H.H.; Yan, F.Q.; Kek, Y.M.; Chew, C.H.; Xu, G.Q.; Ji, W.; Oh, P.S.; Tang, S.H. Synthesis, characterization, and nonlinear optical properties of copper nanoparticles. *Langmuir* **1997**, *13*, 172–175. [[CrossRef](#)]
10. Khodashenas, B.; Ghorbani, H.R. Synthesis of copper nanoparticles: An overview of the various methods. *Korean J. Chem. Eng.* **2014**, *31*, 1105–1109. [[CrossRef](#)]
11. Gu, H.; Chen, X.; Chen, F.; Zhou, X.; Parsaee, Z. Ultrasound-assisted biosynthesis of CuO-NPs using brown alga *Cystoseira trinodis*: Characterization, photocatalytic AOP, DPPH scavenging and antibacterial investigations. *Ultrason. Sonochem.* **2018**, *41*, 109–119. [[CrossRef](#)] [[PubMed](#)]
12. Arya, A.; Gupta, K.; Chundawat, T.S.; Vaya, D. Biogenic synthesis of copper and silver nanoparticles using green alga *Botryococcus braunii* and its antimicrobial activity. *Bioinorg. Chem. Appl.* **2018**, *2018*, 1–10. [[CrossRef](#)] [[PubMed](#)]
13. Ramaswamy, S.V.P.; Narendhran, S.; Sivaraj, R. Potentiating effect of ecofriendly synthesis of copper oxide nanoparticles using brown alga: Antimicrobial and anticancer activities. *Bull. Mater. Sci.* **2016**, *39*, 361–364. [[CrossRef](#)]
14. Abboud, Y.; Saffaj, T.; Chagraoui, A.; El Bouari, A.; Brouzi, K.; Tanane, O.; Ihssane, B. Biosynthesis, characterization and antimicrobial activity of copper oxide nanoparticles (CONPs) produced using brown alga extract (*Bifurcaria bifurcata*). *Appl. Nanosci.* **2013**, *4*, 571–576. [[CrossRef](#)]
15. Bhattacharya, P.; Swarnakar, S.; Ghosh, S.; Majumdar, S.; Banerjee, S. Disinfection of drinking water via algae mediated green synthesized copper oxide nanoparticles and its toxicity evaluation. *J. Environ. Chem. Eng.* **2019**, *7*, 102867. [[CrossRef](#)]
16. Xie, J.; Lee, J.Y.; Wang, D.I.C.; Ting, Y.P. Identification of active biomolecules in the high-yield synthesis of single-crystalline gold nanoplates in algal solutions. *Small* **2007**, *3*, 672–682. [[CrossRef](#)]
17. Saif, S.; Tahir, A.; Asim, T.; Chen, Y. Plant mediated green synthesis of CuO nanoparticles: Comparison of toxicity of engineered and plant mediated CuO nanoparticles towards *Daphnia magna*. *Nanomaterials* **2016**, *6*, 205. [[CrossRef](#)]
18. Yedurkar, S.M.; Maurya, C.B.; Mahanwar, P.A. A biological approach for the synthesis of copper oxide nanoparticles by *Ixora Coccinea* leaf extract. *J. Mater. Environ. Sci.* **2017**, *8*, 1173–1178.
19. Coates, J. Interpretation of infrared spectra, a practical approach. In *Encyclopedia of Analytical Chemistry*; Meyers, R.A., Ed.; John Wiley & Sons Ltd.: Chichester, UK, 2000; pp. 10815–10837.
20. Xu, Y.; Wang, C.; Chen, D.; Jiao, X. Fabrication and characterization of novel nanostructured copper oxide films via a facile solution route. *Mater. Lett.* **2010**, *64*, 249–251. [[CrossRef](#)]
21. Haider, M.J.; Mehdi, M.S. Study of morphology and zeta potential analyzer for the silver nanoparticles. *Int. J. Sci. Eng. Res.* **2014**, *5*, 381–387.
22. Bhaisa, K.C.; D’Souza, S.F. Extracellular biosynthesis of silver nanoparticles using the fungus *Aspergillus fumigatus*. *Colloids Surf. B* **2006**, *47*, 160–164. [[CrossRef](#)]
23. Wu, Y.; Yang, W.; Wang, C.; Hu, J.; Fu, S. Chitosan nanoparticles as a novel delivery system for ammonium glycyrrhizinate. *Int. J. Pharm.* **2005**, *295*, 235–245. [[CrossRef](#)] [[PubMed](#)]
24. Khlebtsov, B.N.; Khlebtsov, N.G. On the measurement of gold nanoparticle sizes by the dynamic light scattering method. *Colloid J.* **2011**, *73*, 118–127. [[CrossRef](#)]

25. Ortiz, J. *Composición Nutricional y Funcional de las Algas Clorofíceas Chilenas: Codium fragile Y Ulva Lactuca*; Universidad de Chile: Santiago, Chile, 2011; Available online: <http://repositorio.uchile.cl/handle/2250/121457> (accessed on 11 October 2020).
26. Ortiz, J.; Uquiche, E.; Robert, P.; Romero, N.; Quítral, V.; Llantén, C. Functional and nutritional value of the Chilean seaweeds *Codium fragile*, *Gracilaria chilensis* and *Macrocystis pyrifera*. *Eur. J. Lipid Sci. Technol.* **2009**, *111*, 320–327. [[CrossRef](#)]
27. Mata, Y.N.; Torres, E.; Blázquez, M.L.; Ballester, A.; González, F.; Muñoz, J.A. Gold(III) biosorption and bioreduction with the brown alga *Fucus vesiculosus*. *J. Hazard. Mater.* **2009**, *166*, 612–618. [[CrossRef](#)]
28. Vijayaraghavan, K.; Mahadevan, A.; Sathishkumar, M.; Pavagadhi, S.; Balasubramanian, R. Biosynthesis of Au(0) from Au(III) via biosorption and bioreduction using brown marine alga *Turbinaria conoides*. *Chem. Eng. J.* **2011**, *167*, 223–227. [[CrossRef](#)]
29. Arockiya Aarthi Rajathi, F.; Parthiban, C.; Ganesh Kumar, V.; Anantharaman, P. Biosynthesis of antibacterial gold nanoparticles using brown alga, *Stoechospermum marginatum* (kützing). *Spectrochimica Acta A Mol. Biomol. Spectrosc.* **2012**, *99*, 166–173. [[CrossRef](#)]
30. Xie, J.; Lee, J.Y.; Wang, D.I.C.; Ting, Y.P. Silver nanoplates: From biological to biomimetic synthesis. *ACS Nano* **2007**, *1*, 429–439. [[CrossRef](#)]
31. Azizi, S.; Ahmad, M.B.; Namvar, F.; Mohamad, R. Green biosynthesis and characterization of zinc oxide nanoparticles using brown marine macroalga *Sargassum muticum* aqueous extract. *Mater. Lett.* **2014**, *116*, 275–277. [[CrossRef](#)]
32. Raveendran, P.; Fu, J.; Wallen, S.L. Completely ‘Green’ Synthesis and Stabilization of Metal Nanoparticles. *J. Am. Chem. Soc.* **2003**, *125*, 13940–13941. [[CrossRef](#)]
33. Wangoo, N.; Bhasin, K.K.; Mehta, S.K.; Suri, C.R. Synthesis and capping of water-dispersed gold nanoparticles by an amino acid: Bioconjugation and binding studies. *J. Colloid Interface Sci.* **2008**, *323*, 247–254. [[CrossRef](#)] [[PubMed](#)]
34. Mandal, S.; Selvakannan, P.R.; Phadtare, S.; Pasricha, R.; Sastry, M. Synthesis of a stable gold hydrosol by the reduction of chloroaurate ions by the amino acid, aspartic acid. *J. Chem. Sci.* **2002**, *114*, 513–520. [[CrossRef](#)]
35. Wang, X.; Zhang, Y.; Song, S.; Yang, X.; Wang, Z.; Jin, R.; Zhang, H. L-Arginine-triggered self-assembly of CeO₂ nanosheaths on palladium nanoparticles in water. *Angewandte Chemie* **2016**, *55*, 4542–4546. [[CrossRef](#)]
36. Zhang, D.; Yang, H. Gelatin-stabilized copper nanoparticles: Synthesis, morphology, and their surface-enhanced Raman scattering properties. *Phys. B Condens. Matter* **2013**, *415*, 44–48. [[CrossRef](#)]
37. Bhagavathy, S.; Sumathi, P.; Bell, I.J.S. Green algae *Chlorococcum humicola*—A new source of bioactive compounds with antimicrobial activity. *Asian Pac. J. Trop. Biomed.* **2011**, *1*, S1–S7. [[CrossRef](#)]
38. Mohseniazar, M.; Barin, M.; Zarredar, H.; Alizadeh, S.; Shanehbandi, D. Potential of microalgae and lactobacilli in biosynthesis of silver nanoparticles. *Bioimpacts* **2011**, *1*, 149–152. [[PubMed](#)]
39. Uma Suganya, K.S.; Govindaraju, K.; Ganesh Kumar, V.; Stalin Dhas, T.; Karthick, V.; Singaravelu, G.; Elanchezhiyan, M. Blue green alga mediated synthesis of gold nanoparticles and its antibacterial efficacy against Gram positive organisms. *Mater. Sci. Eng. C* **2015**, *47*, 351–356. [[CrossRef](#)]
40. Rahimi, Z.; Yousefzadi, M.; Noori, A.; Akbarzadeh, A. Green synthesis of silver nanoparticles using *Ulva flexouosa* from the Persian Gulf, Iran. *JPG* **2014**, *5*, 9–16.
41. Bansal, V.; Rautaray, D.; Ahmad, A.; Sastry, M. Biosynthesis of zirconia nanoparticles using the fungus *Fusarium oxysporum*. *J. Mater. Chem.* **2004**, *14*, 3303–3305. [[CrossRef](#)]
42. Bachar, O.; Meirovich, M.M.; Kurzion, R.; Yehezkeli, O. In vivo and in vitro protein mediated synthesis of palladium nanoparticles for hydrogenation reactions. *Chem. Commun.* **2020**, *56*, 11211–11214. [[CrossRef](#)]